Applied Catalysis B: Environmental 111–112 (2012) 595–604

Contents lists available at SciVerse ScienceDirect

Applied Catalysis B: Environmental

journal homepage: www.elsevier.com/locate/apcatb

Dynamic changes on the surface during the calcination of rapid heat treated TiO_2 photocatalysts

Zs. Pap[a,b], É. Karácsonyi[c], Zs. Cegléd[c], A. Dombi[a], V. Danciu[b], I.C. Popescu[b], L. Baia[d], A. Oszkó[e], K. Mogyorósi[c,*]

[a] Institute of Material Science and Engineering, University of Szeged, Szeged H-6701, P.O. Box 440, Hungary
[b] Faculty of Chemistry and Chemical Engineering, Babes-Bolyai University, Arany János 11, RO-400028 Cluj-Napoca, Romania
[c] Department of Inorganic and Analytical Chemistry, University of Szeged, Dóm tér 7, Szeged H-6720, Hungary
[d] Faculty of Physics, Babes-Bolyai University, M. Kogalniceanu 1, RO-400084 Cluj-Napoca, Romania
[e] University of Szeged, Department of Physical Chemistry and Material Science, Aradi Vt. 1, Szeged H-6720, Hungary

ARTICLE INFO

Article history:
Received 2 May 2011
Received in revised form 3 November 2011
Accepted 6 November 2011
Available online 12 November 2011

Keywords:
Titania
Photocatalysis
Phenol
Rapid crystallization
Surface quality

ABSTRACT

Titanium dioxide photocatalysts were prepared by a newly developed synthesis method that involves rapid heating with short, medium and long exposures of the sol–gel prepared amorphous starting materials (RHSE, RHME and RHLE series) at different temperatures and calcination times. These materials were characterized by various methods, such as XRD, TEM, DRS, IR, nitrogen adsorption and XPS techniques. The detailed study of these catalysts revealed that at low calcination temperatures (e.g. 400 °C) the highest activity will be achieved if a long calcination (90–120 min) is applied because of the surface purification from the deposited organics. At higher temperatures (e.g. 550 °C) shorter calcination times (5–10 min) proved to be effective to achieve high UV activity. At this temperature an unidentified oxygen type was detected from the O1s XPS of the samples which seems to be related to the presence of Ti^{3+}. At 600 °C both short (10 min) and medium calcination (30–90 min) times were found to be beneficial for the phenol degradation under UV irradiation due to the very effective sensitization (10 min of calcination) and surface OH-group preservation (60 min of calcination).

1. Introduction

As titania photocatalysts are more intensively studied, so new synthesis procedures are developed nearly every year. Most of the papers deal with sol–gel prepared photocatalysts, because of the simplicity and high flexibility of this method: wide scale of precursors, including titanium tetraisopropoxide [1–10]; titanium tetraethoxide [11,12]; titanium tetrabutoxide [13–16] and titanium tetrachloride [17]; diversity of the doping sources (i.e. for nitrogen doped titania, triethylamine [1,14], ammonium chloride [2], ammonia [18], ammonium carbonate [3] and urea [13,17]), the possibility of post- [19] or pre-doping [3], etc. The promising results at laboratory scale promoted the industrial production of photocatalysts. Commercial materials, like Evonik Aeroxide P25, Hombikat UV100, Ishira ST-01, etc. appeared already in the early 90s, at the end of 80s (some of them under different name).

However, some synthesis aspects are not yet clarified such as the influence of the calcination parameters on the activity of the photocatalysts. These parameters' optimization could make these catalysts even more inexpensive while retaining their high activity. A good example is the calcination time. Most of the papers apply, 1 [2], 2 [1] or even 6 h [20] of calcination and low heating rates, such as 2 °C/min or 5–10 °C/min [21]. Furthermore, in a few papers, some calcination parameters are missing [22], despite the fact that these works applied the calcination procedure. So, the investigation of at least one of the calcination parameters is required.

The influence of the calcination time was studied only by a few researchers. Joung et al. [23] investigated the effect of the short calcination on nitrogen doped titania and they related the different nitrogen species and calcination times to the obtained trichloroethylene degradation rates. Beydoun and Amal [24] found that the best sucrose decomposition rate of their Fe_2O_3–TiO_2 catalyst was achieved by using only 20 min of calcination at 450 °C.

There are other fields of catalysis in which the inexpensive and highly effective synthesis ways of the nanomaterials are also quite important. A relevant example could be manganese ferrate nanoparticles, which are highly effective catalysts in many chemical processes. High number of publications presents the fine tuning of the same synthesis way for the previously mentioned material, just for obtaining a few percentages of higher stability, or in some cases higher conversion (applied as catalysts) or selectivity [25,26]. As seen above in other fields of materials science is

* Corresponding author. Tel.: +36 62 544 338; fax: +36 62 420 505.
E-mail address: k.mogyorosi@chem.u-szeged.hu (K. Mogyorósi).

0926-3373/$ – see front matter © 2011 Elsevier B.V. All rights reserved.
doi:10.1016/j.apcatb.2011.11.012

rather important to have thorough studies of a single synthesis parameter.

Previously we have proven, that the maximum UV activity of the sol–gel made titanias can be achieved applying very short (10 min) and medium long (60 min) calcination times at 600 °C [27], which means that this aspect is worth investigating at other calcination temperatures by all means. Throughout this work we will try to elucidate what is happening to the titania surface and bulk material at different calcination temperatures and times, by applying rapid heating and short, medium, or long exposures. The photocatalytic activity of these photocatalysts for phenol degradation under UV irradiation will be also evaluated in order to elucidate the influence of the parameters mentioned above.

2. Experimental

2.1. Synthesis of the photocatalysts

TiO_2 samples were synthesized by sol–gel method. 25.0 mL of $TiCl_4$ (Sigma–Aldrich, Purum, ≥98.0%) was added dropwise under vigorous stirring into 50.0 mL of concentrated hydrochloric acid solution (Scharlau, Reagent Grade, 37%). All chemicals were used without further purification. To avoid the overheating of the mixture, the reaction vessel was cooled on an ice bath with the temperature maintained below 5 °C. This mixture was added dropwise under intense stirring into 450.0 mL of high purity Milli-Q water. Subsequently 7.8 mL of glacial acetic acid was also added dropwise. The pH 8 was adjusted with an aqueous solution of ammonia (25%). The mixture was left for 2 days at room temperature to complete the hydrolysis. The precipitate was dried at 80 °C for 24 h and the resultant white powder was milled.

This amorphous powder was calcinated by heating in a quartz boat placed within a quartz tube in a tubular furnace under still air. A special heat treatment procedure was applied in which the temperature of the amorphous material was raised to the desired calcination temperature in a short time applying high heating rate in three subsequent steps (60, 20 and 10 °C/min). Their value was decreased as the temperature reached the threshold to prevent the overheating of the furnace. The studied calcination temperatures were: 400 °C, 500 °C, 550 °C and 600 °C, with calcination times of 5, 7.5, 10, 12, 15, 20, 30, 60, 90, 120 and 180 min at the given temperature. The gaseous thermal decomposition by-products were purged from the system by air in the last minute of the calcination procedure. The obtained samples were washed and centrifuged in Milli-Q water or in ethanol–water mixture (50:50%, v/v, 0.8 g product/50 mL) three times in order to remove any soluble impurities. The powder was finally dispersed in Milli-Q water and irradiated in a Petri dish with UV irradiation (λ = 365 nm) to remove any organic traces from the TiO_2 samples.

The coding of the materials followed the heating mode-temperature-calcination time scheme (e.g. RHSE-400-10). The samples synthesized by the rapid heating up and short exposure (5–20 min) procedure were named RHSE (for further details see [27]), the samples calcined at 30 and 60 min were coded RHME (rapid heating medium exposure); the samples calcined longer than 60 min (90, 120 and 180) were coded RHLE (rapid heating long exposure). The nanomaterials obtained using slow heating and long exposure were coded SHLE. The presence of the "w" prefix means that the amorphous material was washed before calcination (for e.g. wRHSE-600-10).

2.2. Characterization methods and instrumentation

X-ray diffraction (XRD) measurements were performed on a Rigaku diffractometer using Cu-Kα radiation (λ = 1.5406 Å), equipped with a graphite monochromator. The anatase–rutile phase ratio was evaluated using the method developed by Zhang and Banfield [28], and the crystallites average size was calculated using the Scherrer equation [29].

Transmission electron microscopic (TEM) measurements were executed to characterize the crystallite size, distribution and also to identify the morphology of the particles. TEM micrographs were recorded on a Philips CM 10 instrument operating at 100 kV using Formvar coated copper grids.

The specific surface area of the catalysts was determined by nitrogen adsorption at 77 K by a Micromeritics gas adsorption analyzer (Gemini Type 2375). The specific surface area was calculated using the BET method.

JASCO-V650 spectrophotometer with an integration sphere (ILV-724) was used for measuring the DRS (diffuse reflectance spectroscopy) spectra of the samples (λ = 220–800 nm).

The FT-IR spectra were recorded by using a Bruker Equinox 55 spectrometer with an integrated FRA 106 Raman module using a Nd–YAG laser (1064 nm). Measurements were recorded with a power incident of 300 mW and a spectral resolution of 1 cm^{-1}. Samples were ground with KBr pressed into thin pellets (thickness ~ 0.3 mm) and IR spectra were recorded with a spectral resolution of 2 cm^{-1}. For the data analysis and peak separation Origin and eXPFit by Dr. Roger Nix for Microsoft Office Excel add-in were used.

X-ray photoelectron spectra (XPS) of selected samples were taken with a SPECS instrument equipped with a PHOIBOS 150 MCD 9 hemispherical electron energy analyzer operated in the FAT mode. The excitation source was the K_α radiation of a magnesium anode ($h\nu$ = 1253.6 eV). The X-ray gun was operated at 180 W (12 kV, 15 mA). The pass energy was set to 20 eV, the step size was 25 meV, and the collection time in one channel was 150 ms. Typically five scans were added to get a single spectrum. The C1s binding energy of adventitious carbon (285.1 eV) was used to calibrate the energy scale. Data acquisition and analysis was performed using both the manufacturer's (SpecsLab2) and commercial (CasaXPS, Origin) software and before data analysis X-ray satellites, originating from the non-monochromatic excitation source, were removed from the spectra.

The heat treatment of the amorphous titania was executed in a tubular furnace (Thermolyne 21100, total length 38 cm, quartz tube length 64 cm, tube interior diameter 5.5 cm, quartz tube diameter 4 cm).

2.3. Determination of the photocatalytic activities

A Heraeus type photoreactor system with a TQ-150 high pressure mercury lamp (λ > 310 nm) was used to measure photocatalytic activity. The photocatalyst suspension containing phenol ($c_{0,substrate}$ = 0.5 mM, c_{TiO_2} = 1.0 g/L, V_{susp} = 400 mL) was continuously purged by air 40 L/h in order to maintain a constant concentration of dissolved oxygen during the irradiation. The concentration decrease of the chosen pollutant (phenol) was followed as described in our previous work [27].

The initial rate of the photocatalytic degradation of the model compound, r_0 was considered to evaluate the efficiency of the photocatalyst. To determine r_0, an empirical function was fitted to the experimentally observed data points with the initial rate determined from the slope when t = 0.

Evonik Aeroxide P25 (P25 later on) TiO_2 (89 wt% anatase, 11 wt% rutile and ~50 m^2/g specific surface area) was chosen as one of the reference catalysts. The wSHLE-450-180 sample was used as a sol–gel reference material (prepared using the method developed by Xu et al. [30]) to highlight the importance of the rapid heating and short exposure times and to emphasize the major difference

between conventional heat treatment and the rapid crystallization procedure.

3. Results and discussion

3.1. Characterization of the photocatalysts[1]

The first step in the characterization of the materials was to determine their crystal phase composition. Based on the XRD patterns (Fig. 1a–c), the following crystal phases were identified: anatase, rutile and brookite. Anatase was present in all samples in different amounts, depending on the heat treatment temperature: ~100 wt% in the samples treated at 400 °C, 84–88 wt% in the samples treated at 550 °C and 78–82 wt% in the samples calcined at 600 °C (Table 1 and Fig. 1a–c). As the heat treatment temperature increases so does the rutile's ratio in the samples. The presence of brookite was negligible (below 1 wt%) in the samples obtained at 400 and 550 °C and totally absent from the materials calcined at 600 °C.

As expected, the calculated primary crystallite size also increased in conjunction with the heat treatment temperature. At 400 °C the anatase crystallite's size was 12.6 nm. At 550 °C this value reached 26.6 nm and finally 41.4 nm at 600 °C. The rutile crystallite size was between 90 and 100 nm, which is considerably larger than that determined for anatase particles (Table 1). Caution should be taken when analyzing larger crystallite size (>50 nm) from line broadening as equipment inaccuracies may become significant. The crystallite size calculated from XRD is in good agreement with the crystallite size values determined by TEM imaging (see Fig. 2).

The DRS spectra of the representative samples were recorded in order to evaluate the importance of the light absorption in the photocatalytic performance of the samples. The majority of the materials calcined at 400, 550 and 600 °C showed an absorption shoulder from 400 to 525 nm. As Fig. 3a–c shows, the light absorption of the photocatalysts decreases as the calcination time gets longer.

The small primary crystallite size may point out possible visible light active catalysts, as showed by Ryu and Choi [31] and the DRS spectra could give some hints about possible doping [32] or sensitizing [13]. However these two key parameters were unable to explain the observed photocatalytic activities (Fig. 4), thus a detailed study about the surface of these materials by other methods (such as IR spectroscopy and XPS) was needed.

3.2. Correlations observed between the surface quality, bulk properties and the achieved photocatalytic performance

3.2.1. Samples heat treated at 400 °C

The phenol degradation rates observed for these catalysts were below the degradation rate measured with P25 (20.5×10^{-8} mol dm^{-3} s^{-1}). The best performing catalyst was obtained at 120 min of calcination while the samples treated for 5 up to 60 min were the least active from this series (Figs. 4 and 5a). All the materials in this series (except RHLE-400-120 and RHLE-400-180 sample) were unable to exceed the performance of the sol–gel reference sample, wSHLE-450-180. These experimental data can raise the following questions:

(i) What causes the low activity at shorter calcination times?

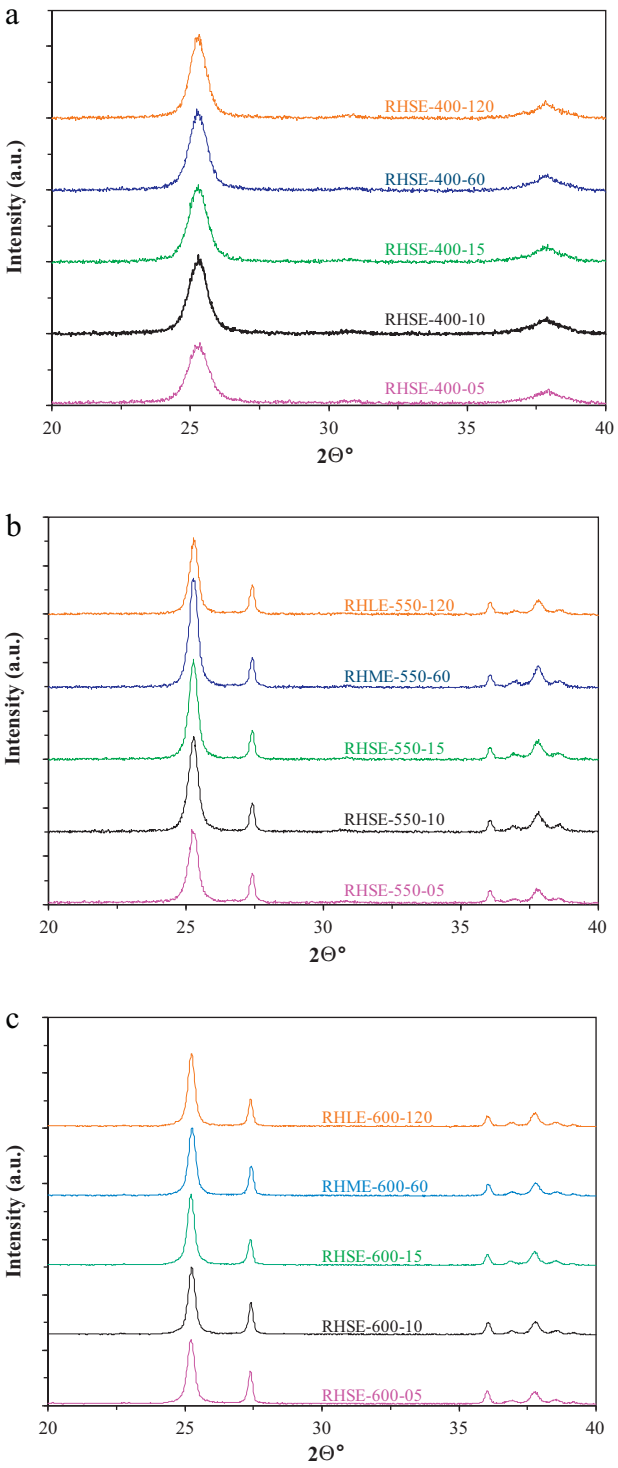

Fig. 1. (a) XRD pattern of samples treated at 400 °C. (b) XRD pattern of samples treated at 550 °C. (c) XRD pattern of samples treated at 600 °C.

(ii) What is the reason for the activity maximum at 120 min of calcination?

It was concluded that all samples from the 400 °C series have practically the same phase composition, primary crystallite size (Fig. 1a and Table 1) and practically, the same specific surface area. We also observed that while the heat treatment time increases the absorbance at 425–475 nm decreases (Fig. 3a). This obviously

[1] Please note that this paper will discuss those samples that revealed critical information about the evolution of the catalyst's surface quality and other bulk properties (these samples were treated at 400, 550 and 600 °C). However Fig. 4 contains the degradation data of all the measured samples.

Table 1
Crystal phase composition and primary crystallite size of the key samples calcined at 400, 550 and 600 °C.

Sample name	Anatase (wt%)	Rutile (wt%)	Brookite (wt%)	d_A (nm)	d_R (nm)	S_{BET} (m^2/g)
RHSE-400-05	100	–	Trace amounts	10.6	–	
RHSE-400-10	100	–		12.6	–	63.6
RHSE-400-15	100	–		12.4	–	
RHME-400-60	100	–		12.9	–	
RHLE-400-120	100	–		14.5	–	
RHSE-550-05	88.2	11.8	Trace amounts	26.6	~85	
RHSE-550-10	86.5	13.5		22.4	~86	36.0
RHSE-550-15	84.2	15.8		30.2	~89	
RHME-550-60	85.3	14.7		29.8	~90	
RHLE-550-120	85.4	14.6		33.5	~86	
RHSE-600-05	77.8	22.2	–	38.8	~95	
RHSE-600-10	82.4	17.6		41.4	~95	16.1
RHSE-600-15	81.5	18.5		41.8	~95	
RHME-600-60	79.6	20.4		41.2	~99	
RHME-600-120	80.0	20.0		40.4	~100	
Aeroxide P25	89.0	11.0	–	26.0	~85	50.0
wSHLE-450-180	100	–	–	16.7	–	60.0

means that the surface quality of the catalyst is slowly changing with the heat treatment time.

The X-ray photoelectron spectra, surprisingly showed that no changes could be determined in the type of nitrogen incorporation (O–Ti–N, interstitial type [33]) and concentration between the samples in this series (~1.0 ± 0.1 at.%). Similarly no changes were observed in the Ti:O ratio. The carbon deposits detected on the surface decreased slowly throughout the calcination time (5–180 min) that indicating a very slow surface purification which could explain the higher UV activity at longer calcination times.

At very short treatment times (5–10 min), ~7 at.% of all oxygen forms in the surface layer can be found as surface OH-groups and the remaining part exists as oxide. However, after 120 min of calcination this value decreases to ~6 at.%, so a slight dehydroxylation can be observed. This observation suggests that the samples treated for longer times should exhibit slightly lower phenol degradation rates as we have previously found [27], thus further examination is needed to explain the activity maximum at 120 min.

A possible reason for this can be found in the IR spectra of these materials. In Fig. 6 is clearly visible that two overlapped absorption bands were detected in the RHSE-400-05 sample. After peak separation the two bands are clearly visible. The first one at 1615 cm^{-1} can be identified as $-NH_2$ and the band at 1635–1640 cm^{-1} corresponds indirectly to the surface –OH-groups [34]. The presence of NH_2-group is not surprising at all, if we know that our samples contained a substantial quantity of ammonium salts. As the calcination time increases these bands ratio and intensity changes simultaneously. At short and medium calcination (5–60 min) times the NH_2 and OH bands are both intense. However, at long calcination times the first band nearly disappears, the second one becomes wider and less intense (Fig. 7). This observation confirms the surface dehydroxylation observed from the XPS. The OH band vanishes (as in the case of wSHLE-450-180, Fig. 8) from the sample treated at 180 min (RHLE-400-180), which could explain [35] the observed lower UV activity (compared to the sample RHLE-400-120).

However the presence of the surface anchored NH_2-groups could be important, because it is possible, that the low activity of the

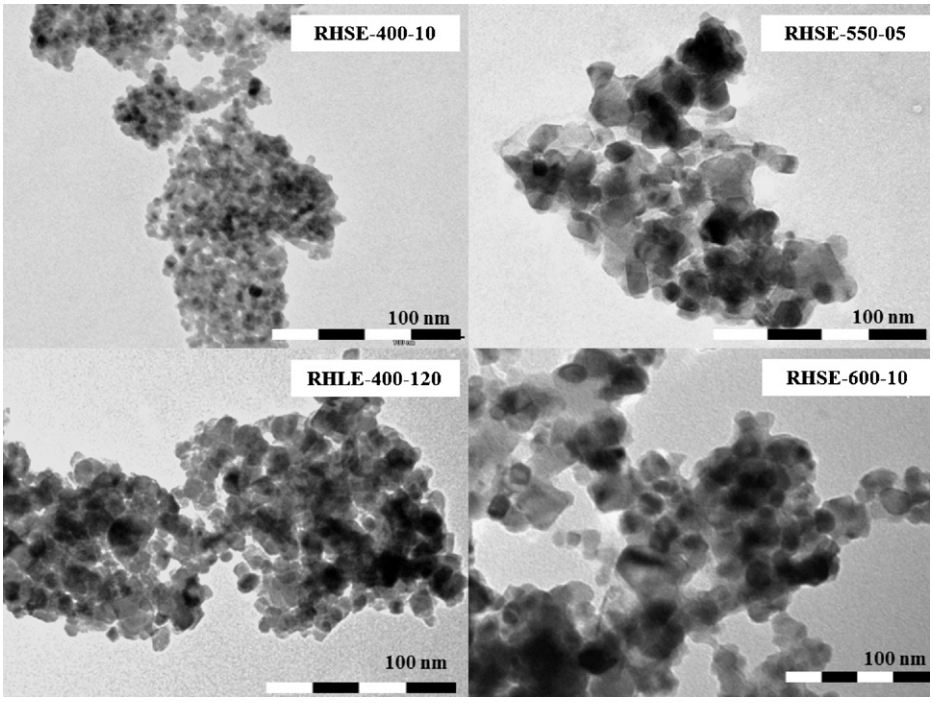

Fig. 2. TEM micrographs of RHSE-400-10, RHLE-400-120, RHSE-550-05 and RHSE-600-10 samples.

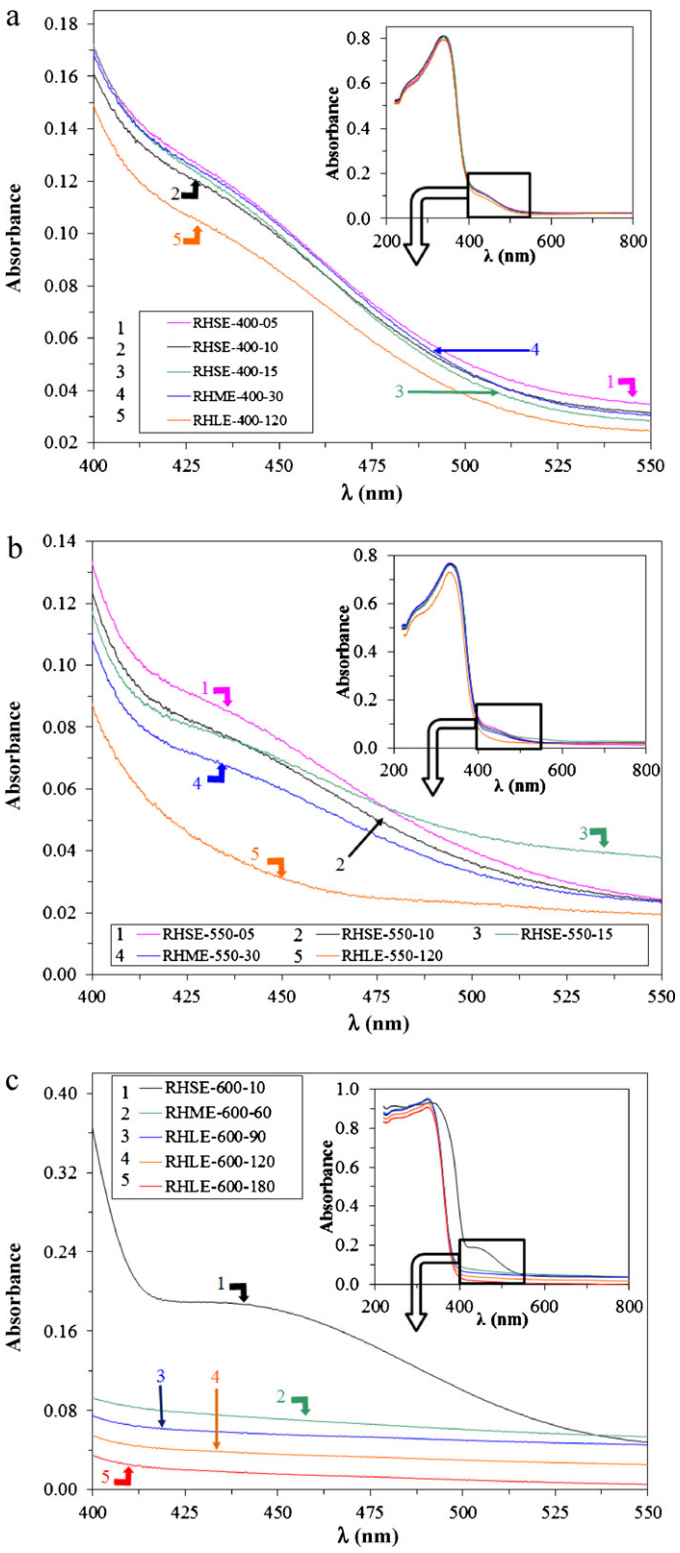

Fig. 3. (a) DRS spectra of samples treated at 400 °C. (b) DRS spectra of samples treated at 550 °C. (c) DRS spectra of samples treated at 600 °C.

samples calcined at shorter times can be attributed to pure visible light activity (here the NH_2-group can act as a sensitizer [36]). This theory needs further investigations based on experiments carried out under visible light.

Very interesting bands were observed at 2854 cm^{-1} and 2924 cm^{-1} (Fig. 9). These bands can be assigned to long chained hydrocarbons (similar to those observed by Lettmann et al. [37]).

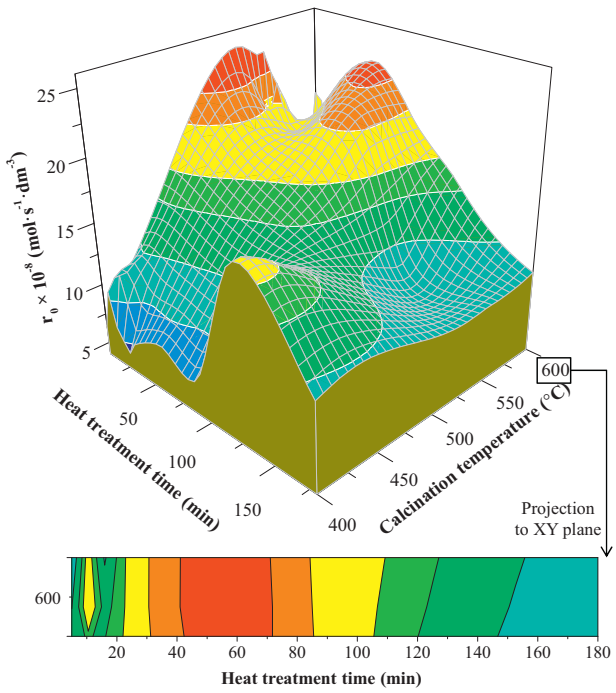

Fig. 4. The optimization of the photocatalytic activity of the titania samples as function of the heat treatment time and temperature. A separate projection was attached to reveal the maximum at 600 °C and 10 min of calcination otherwise covered in the original surface plot.

Their presence indicates that the surface of all investigated catalysts in this series is covered by organic residues. The intensity of these bands decreases throughout the calcination series as the heat treatment time increases, in parallel with the intensity of the NH_2 and OH bands and the UV–vis absorption. Unfortunately, no other obvious correlation was found between these bands and the measured photocatalytic activity in this series.

3.2.2. *Samples heat treated at 550 °C*

The phenol degradation rates measured for these samples were slightly below the P25's degradation rate, except for one (Figs. 4 and 5b). The best performing catalyst was obtained at 5 min of heat treatment and exceeded by 5% the activity of P25. All the materials were performing better than the sol–gel reference sample (wSHLE-450-180), except RHLE-550-180. This fact confirms the assumption that for high UV photocatalytic performance, higher calcination temperatures are recommended. The following points should be clarified:

(i) The unusually high activity for sample RHSE-550-05.
(ii) The significant activity decrease observed in this series (from $\sim 25 \times 10^{-8}$ mol dm^{-3} s^{-1}, sample RHSE-550-05 to 9×10^{-8} mol dm^{-3} s^{-1}, sample RHLE-550-180).

We know that all samples in the 550 °C series have practically the same phase composition, primary crystallite size (Fig. 1b and Table 1) and same specific surface area (same behavior was observed for the samples treated at lower temperatures, see the previous section). It was also noticed that while the heat treatment time increases the considerable absorbance at 425–475 nm decreases (Fig. 3b) – as it was similarly found for the series of samples treated at 400 °C. This obviously means that the surface quality of the catalyst is slowly changing throughout the heat treatment time.

It is rather unusual for a sample that is treated only for 5 min to have such high photocatalytic activity. One of the possible answers

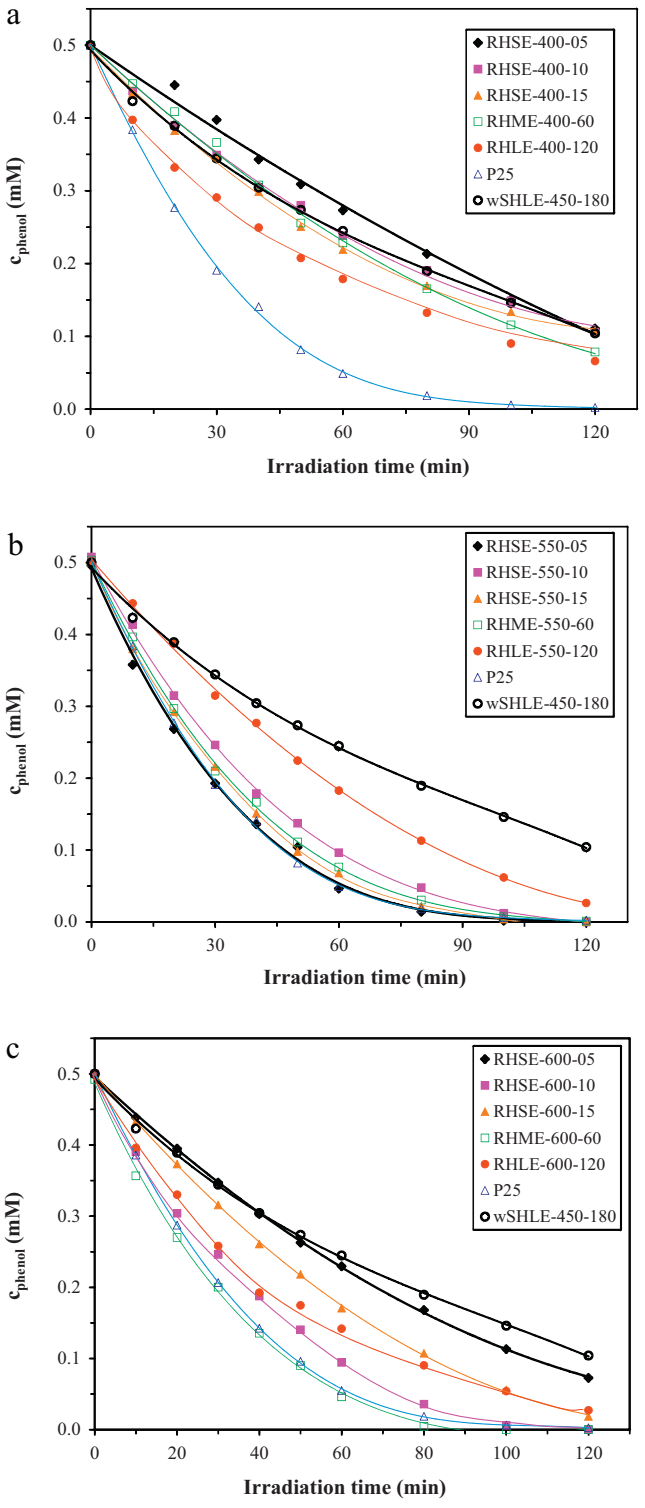

Fig. 5. (a) Phenol decomposition on samples treated at 400 °C. (b) Phenol decomposition on samples treated at 550 °C. (c) Phenol decomposition on samples treated at 600 °C.

is given by the XPS. The total amount of nitrogen measured in this sample was 1.2 at.%. First of all the nitrogen type detected is substitutional [38] (88 at.% from the total nitrogen) and a small amount of interstitial nitrogen (12 at.% from the total nitrogen) incorporation was also found (Fig. 10). The formation of the substitutional nitrogen is favored when the crystallization occurs under oxygen poor conditions [38], like in our case. Surprisingly, disappears in the

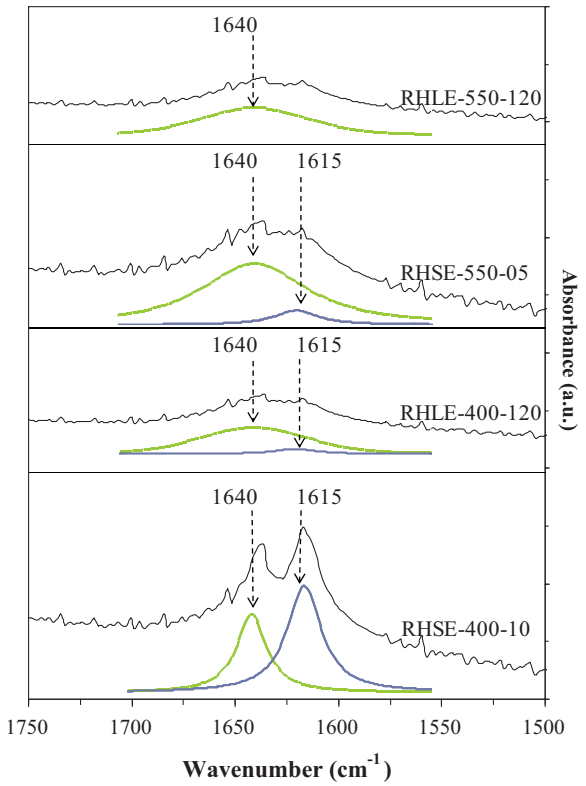

Fig. 6. IR spectra (region 1500–1750 cm^{-1}) of sample RHSE-400-05, RHLE-400-120, RHSE-550-05 and RHLE-550-120.

samples calcined for longer times, at this temperature, and only a small amount of interstitial nitrogen remains in 0.7 at.%. As the calcination time extends so the nitrogen leaves the substitutional position possibly as elemental nitrogen or a rearrangement occurs as interstitial nitrogen.

Furthermore at ~458 eV a small amount of Ti^{3+} (1 at.% from the total titanium, 0.02 at.% from the atomic total) was detected (Fig. 11) concomitantly with an unidentified oxygen type at ~528 eV (5.7 at.% from the total oxygen and 1.7 at.% from the atomic total, see Fig. 12). These two species disappear simultaneously as the calcination time advances. It is very important to elucidate the relationship between Ti^{3+} and the unidentified oxygen type. In order to clarify this question properly we should consider the following facts:

(i) Yang et al. [39] predicted in their work that along Ti^{3+} sites there must be a change in the oxygen types in their $TiO_{2-x-y}N_xC_y$ films.
(ii) If Ti^{3+} is present in a given system (in our case in the TiO_2 crystal), than a change is observable in oxygen photoelectron spectra towards lower binding energies [40].
(iii) The formation of oxygen vacancies is favored by substitutional nitrogen doping [41].
(iv) The presence of Ti^{3+} is simultaneous with the existence of oxygen vacancies [42].

Based upon the listed points it is clear that the substitutional nitrogen doping is related to the presence of Ti^{3+} and oxygen defects which are indirectly visible via the presence of the lower binding energy type of oxygen. This could have a major impact on the measured photocatalytic activity as we observed in our previous work [43]. In that paper we noticed in our flame made titania samples the same oxygen type (3 at.% from the oxygen total), especially in the highly active samples. In the low activity catalysts

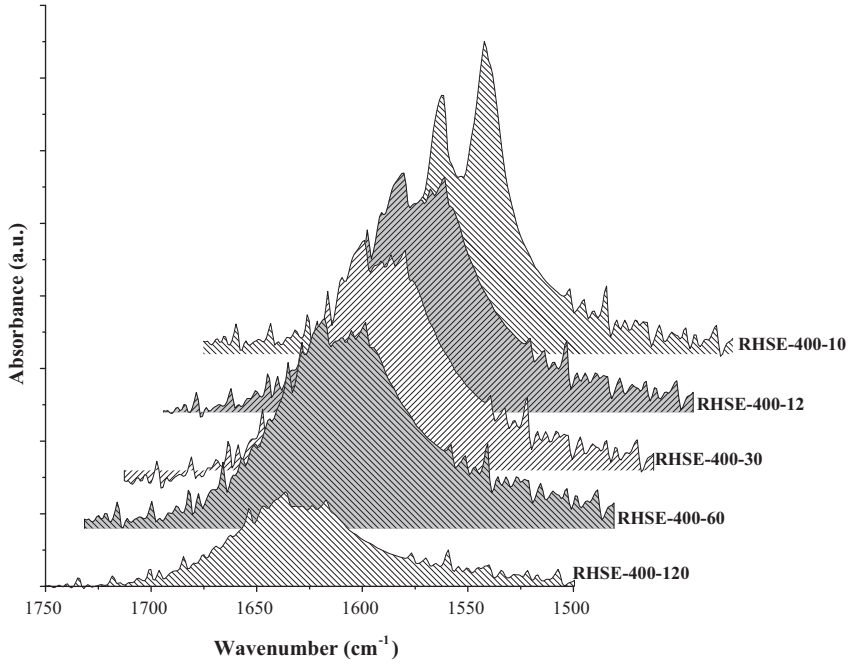

Fig. 7. IR spectra of several selected samples calcined at 400 °C (region 1500–1750 cm^{-1}).

no such oxygen type was detected. However in the best materials no Ti^{3+} was detected concomitantly with the lower binding energy type of oxygen, possibly because of its low concentration, below the detection level, or their accumulation in the deeper layers.

The IR spectra of these samples reveal important information and changes compared to the samples treated at lower temperatures. The NH_2 band is still visible in the RHSE-550-05 sample at 1615 cm^{-1} (Fig. 6), but is significantly weaker than in the samples calcined at 400 °C. The OH band at 1635–1640 cm^{-1} becomes dominant in this series. In the RHLE-550-120 sample the NH_2 signal is missing, thus we can affirm that no more ammonia residues could be found on the surface. This is indirectly observable also from the DRS spectra (Fig. 3b). The activity decrease throughout the series can be explained by the surface dehydroxylation and the continuous decrease of the light absorbance in the 425–475 nm range. The carbon content remained low in all the samples in this series. The bands at 2854 cm^{-1} and 2924 cm^{-1} indicate that the long chained hydrocarbons are constantly present at the catalyst's surface (Fig. 9). Their intensity decrease is accompanied by the absorbance decrease in the DRS spectra, the disappearance of the NH_2-band and the intensity decrease of OH band.

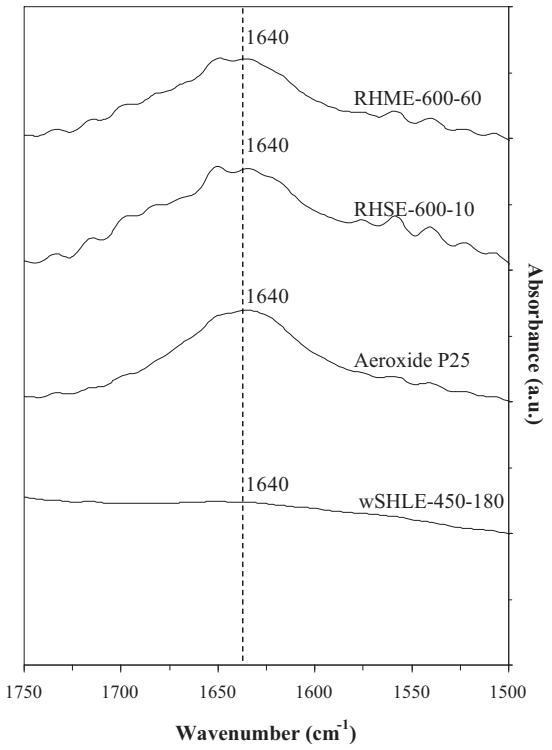

Fig. 8. IR spectra of sample wSHLE-450-180, Aeroxide P25, RHSE-600-10 and RHME-600-60 (region 1500–1750 cm^{-1}).

3.2.3. Samples treated at 600 °C

The phenol degradation rates measured for these samples were between 50% (sample RHLE-600-180) and 115% (sample RHME-600-60) of P25's degradation rate, except for sample RHSE-600-180. Another activity maximum (90% of P25's activity) was observed at 10 min of calcination (sample RHSE-600-10) (Figs. 4 and 5c). All the materials were performing better than the sol–gel reference sample (wSHLE-450-180). Some interesting observations could be made related to:

(i) The high activity of the samples RHSE-600-10 and RHME-600-60.
(ii) The reason for the high activity for the sample RHSE-600-10.

We observed that all the samples from the 600 °C series have the same phase composition, primary crystallite size (Table 1) and same specific surface area (same behavior was observed for the samples treated at lower temperatures, see the previous two sections). We also noticed the fact that while the heat treatment time increases the considerable absorbance at 425–475 nm decreases (Fig. 3c) – also observed in the previous two cases.

The XPS of the catalysts in this series showed that no nitrogen incorporation occurred, thus we can affirm that nitrogen doping is nearly impossible at this temperature. However, the same unidentified oxygen type was observed at ~528 eV (Fig. 13) in the highly

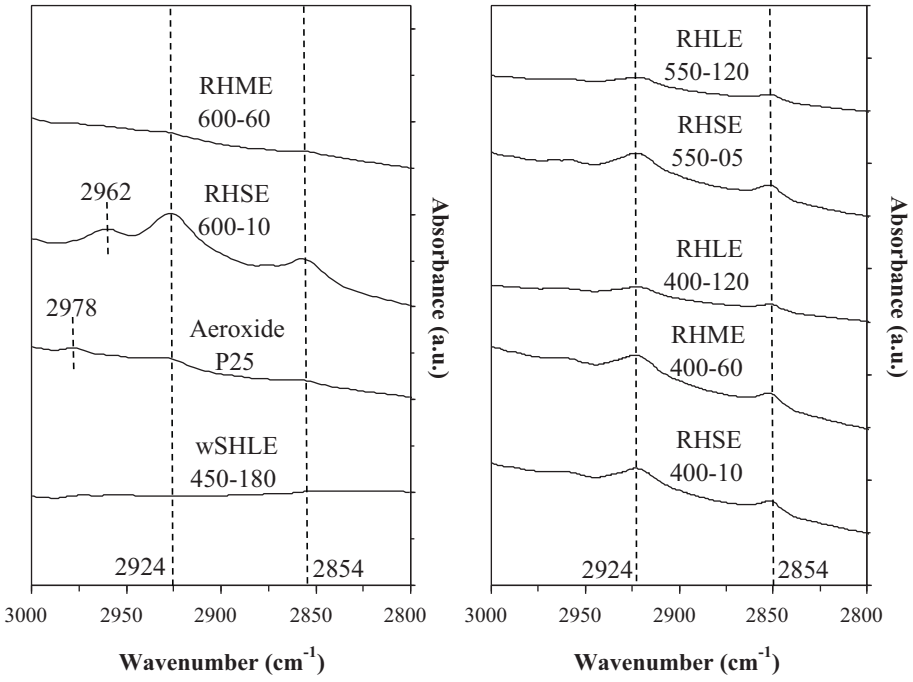

Fig. 9. IR spectra of the most significant samples (region 2800–3000 cm^{-1}).

active samples. In the materials treated for longer times this special oxygen type is missing. The observed concentration of this type of oxygen in sample RHME-600-60 was ~2.6 at.% from the oxygen total (compared to the ~5.7 at.% in sample RHSE-550-05). The same quantity was found in sample RHSE-600-10. We did not observe any Ti^{3+} sites, probably due to its low concentration. Also a slight dehydroxylation was observed in this series (as in the case of the samples calcined at lower temperatures). Based upon the O1s XPS of the samples, two activity maxima cannot be explained.

Fig. 8 shows the IR spectra for three highly active samples (P25 B, RHSE-600-10, and RHME-600-60) and the sol–gel reference, wSHLE-450-180 sample. The highly active photocatalysts all have very similar surface OH-group absorption bands at

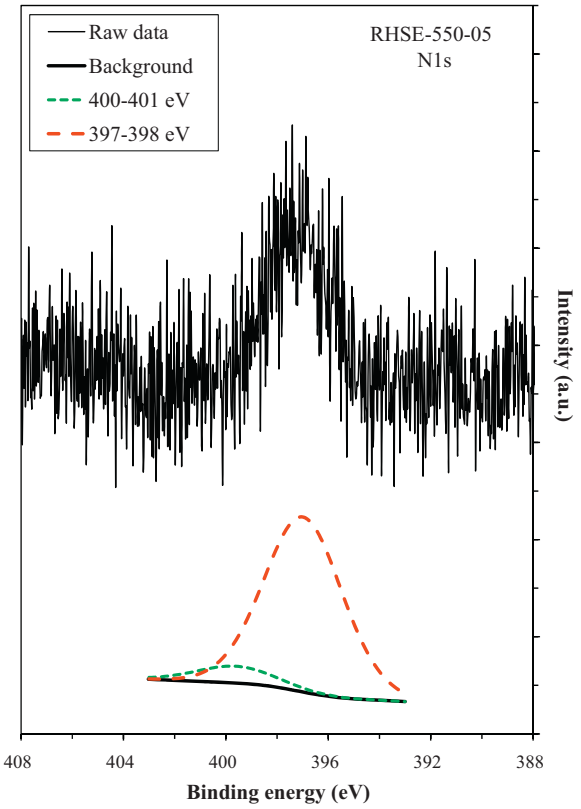

Fig. 10. XPS N1s signal for sample RHSE-550-05.

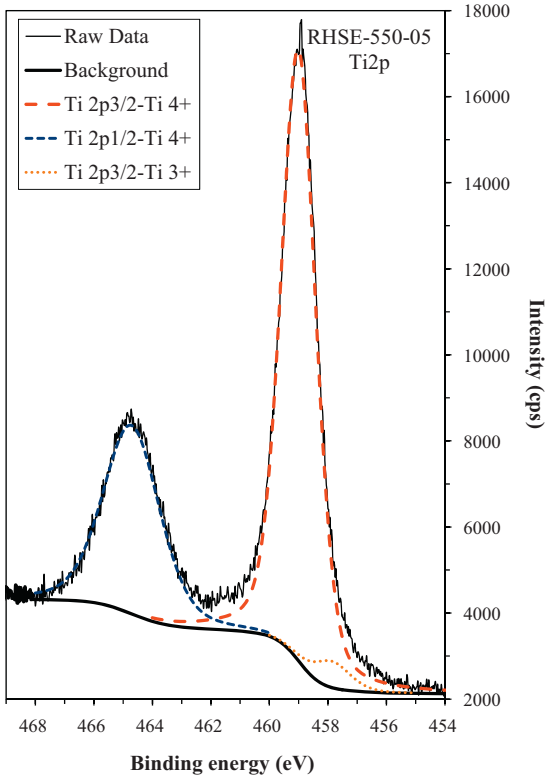

Fig. 11. XPS Ti2p signal for sample RHSE-550-05.

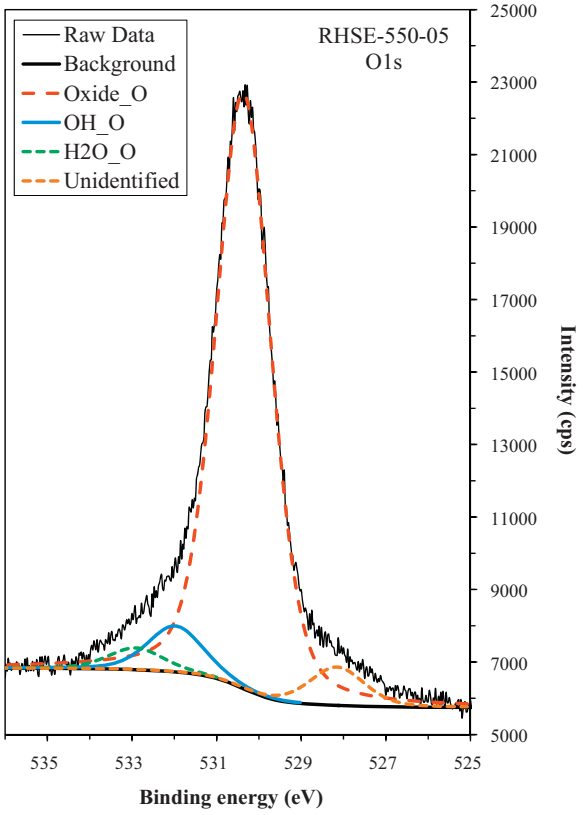

Fig. 12. XPS O1s signal for sample RHSE-550-05.

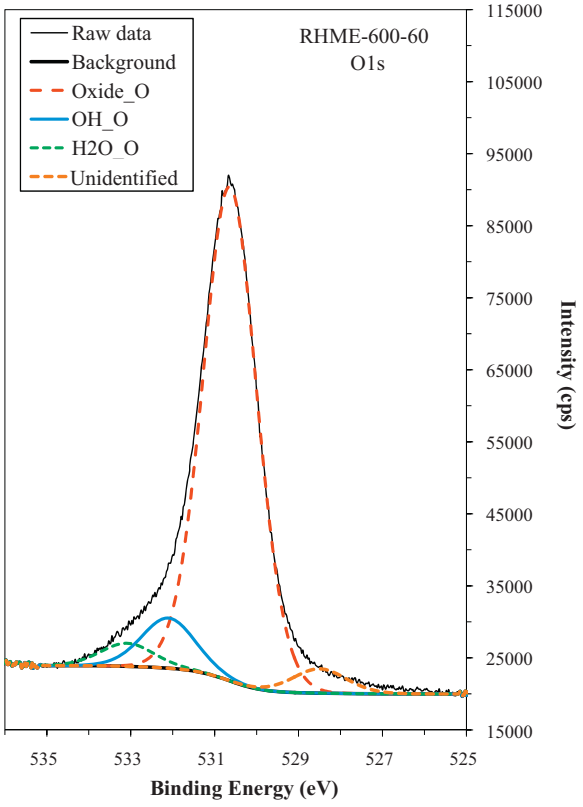

Fig. 13. XPS O1s signal for sample RHME-600-60.

1635–1640 cm^{-1} while there is no corresponding absorption for the wSHLE-450-180 sample. No NH_2 bands were observed in the materials of this series. The loss of surface OH-groups in the traditionally calcined material, which is assumed to occur during long time calcination, could be one of the main reasons for the low UV activity.

The spectrum of RHSE-600-10 sample shows several small bands at ~2870 cm^{-1} while the RHME-600-60 sample lacks this feature (Fig. 9). These absorptions arise from long hydrocarbons chains and this means that after a short calcination time, carbonaceous species (–C–C–) still could remain on the catalyst's surface, similarly to the materials calcined at lower temperatures (Fig. 9) [37]. These species may cause a small red shift and a visible light absorption in the 420–530 nm range in the DRS spectra of the catalysts and may be the origin of the yellow color of RHSE-600-10 sample (Fig. 3c). This shift and extra absorption could sensitize the photocatalyst to be excited over a broader spectral range of the irradiation. In fact at this temperature a plus absorption band appears in the 2800–3000 cm^{-1} region at 2962 cm^{-1}, which could be the reason for the successful sensitization.

Although this effect could increase the photocatalytic activity, too much organic impurities remaining on the surface are obviously disadvantageous for photocatalytic purposes. Longer calcination times cause the thermal decomposition of these organic species, possibly forming first an amorphous carbon layer on the nanocrystals (minimum local activity at RHSE-600-20) and finally a virtually carbon-free clean surface as in case of sample RHME-600-60.

Fig. 4 clearly shows that the samples obtained using longer calcination times (30–120 min) have higher activity than those calcined for very short times (5–15 min). The only exception is the sample treated for 10 min with its unexpectedly high activity probably due to the sensitization of the photocatalyst. Long heat treatment times (120–180 min) can cause a drastic activity decrease.

4. Conclusions

The literature regarding sol–gel prepared titanias, treated the calcination as a standard procedure without seriously considering its complex influence on the photocatalytic properties on the obtained nanomaterials. It is well known how the temperature can modify the primary crystallite size and phase composition but no meticulous study was published regarding the influence of the calcination time.

We have successfully shown that in a temperature series, throughout the calcination times several surface parameters change continuously, like: the presence of NH_2-group at lower temperatures, the influence of the long chained hydrocarbons, the dehydroxylation phenomena, the nitrogen incorporation, the evolution of the light absorption of the samples, etc. Several evidences were brought up to support the role of each surface parameter.

It was proven that very active catalysts can be made with just 5 (RHSE-550-05 sample) or 10 (RHSE-600-10 sample) min of calcination and experimental data were collected to explain their unusual properties. However, in some cases (RHME-600-60 and RHLE-400-120 samples) due to the longer calcination time a surface purification occurs and a photoactivity increase was observed. We demonstrated that at low calcination temperature, because of the surface coverage with organic residues/carbon deposits, only low UV activity can be obtained.

The samples treated at higher temperatures (above 500 °C) were more active than the sol–gel reference wSHLE-450-180 sample and only a few samples, such as RHSE-550-05 and RHME-600-60 exceeded the performance of the well-known Evonik Aeroxide P25.

Acknowledgements

This article has been produced with the financial assistance of the European Union (Hungary-Serbia IPA Cross-border Co-operation Programme; HU-SRB/0901/121/116). The content of the document is the sole responsibility of the University of Szeged and can under no circumstances be regarded as reflecting the position of the European Union and/or the Managing Authority.

This work was co-financed by the grant from Swiss Contribution (SH/7/2/20) and by the grant from the Hungarian National Office of Research and Technology (OTKA CK 80193). Authors thank for the Hungarian-Romanian TeT mobility project (OMFB-00415/2008/RO-21/2007). KM thanks the financial support of the Hungarian Research Foundation (OTKA PD78378) and the János Bolyai Research Scholarship of the Hungarian Academy of Sciences.

The authors are indebted to Evonik Industries for supporting our work by supplying Aeroxide P25 TiO_2 sample for these studies.

References

[1] G. Liu, X. Wang, L. Wang, Z. Chen, F. Li, G.Q. Lu, H.M. Cheng, J. Colloid Interface Sci. 334 (2009) 171–175.
[2] S. Livraghi, A.M. Czoska, M.C. Paganini, E. Giamello, J. Solid State Chem. 182 (2009) 160–164.
[3] X. Zhang, Q. Liu, Appl. Surf. Sci. 254 (2008) 4780–4785.
[4] K. Katsumata, A. Nakajima, N. Yoshida, T. Watanabe, Y. Kameshima, K. Okada, Surf. Sci. 596 (2005) 197–205.
[5] Y.V. Kolenko, A.V. Garshev, B.R. Churagulov, S. Boujday, P. Portes, C.C. Justin, J. Photochem. Photobiol. A 172 (2005) 19–26.
[6] T. Sreethawong, Y. Suzuki, S. Yoshikawa, J. Solid State Chem. 178 (2005) 329–338.
[7] L. Miao, S. Tanemura, S. Toh, K. Kaneko, M. Tanemura, Appl. Surf. Sci. 238 (2004) 175–179.
[8] Y. Bessekhouad, D. Robert, J.V. Weber, N. Chaoui, J. Photochem. Photobiol. A 167 (2004) 49–57.
[9] S. Boujday, F. Wünsch, P. Portes, J.F. Bocquet, C.C. Justin, Sol. Energy Mater. Sol. Cells 83 (2004) 421–433.
[10] J.A. Wang, A. Cuan, J. Salmones, N. Nava, S. Castillo, M.M. Pineda, F. Rojas, Appl. Surf. Sci. 230 (2004) 94–105.
[11] X. Qiu, C. Burda, Chem. Phys. 339 (2007) 1–10.
[12] J. Widoniak, S.E. Assmann, G. Maret, Colloids Surf. A 270–271 (2005) 329–334.
[13] D. Chen, D. Yang, J. Geng, J. Zhu, Z. Jiang, Appl. Surf. Sci. 255 (2008) 2879–2884.
[14] D.G. Huang, S.J. Liao, J.M. Liu, Z. Dang, L. Petrik, J. Photochem. Photobiol. A 184 (2006) 282–288.
[15] M. Zamora, T. López, R. Gómez, M. Asomoza, R. Meléndrez, Appl. Surf. Sci. 252 (2005) 828–832.
[16] Z. Li, B. Hou, Y. Xu, D. Wu, Y. Sun, W. Hu, F. Deng, J. Solid State Chem. 178 (2005) 1395–1405.
[17] J. Yuan, M. Chen, J. Shi, W. Shangguan, Int. J. Hydrogen Energy 31 (2006) 1326–1331.
[18] L. Mi, P. Xu, P.N. Wang, Appl. Surf. Sci. 255 (2008) 2574–2580.
[19] J.A. Rengifo-Herrera, J. Kiwi, C. Pulgarin, J. Photochem. Photobiol. A 205 (2009) 109–115.
[20] D.G. Huang, S.J. Liao, J.M. Liu, Z. Dang, L. Petrik, J. Photochem. Photobiol. A: Chem. 184 (2006) 282–288.
[21] P. Sampedro, G. Colón, M.F. García, J. Photochem. Photobiol. A: Chem. 199 (2008) 136–143.
[22] D.L. Liao, G.S. Wu, B.Q. Liao, Colloids Surf. A 348 (2009) 270–275.
[23] S.K. Joung, T. Amemiya, M. Murabayashi, K. Itoh, Appl. Catal. A 312 (2006) 20–26.
[24] D. Beydoun, R. Amal, Mater. Sci. Eng. B 94 (2002) 71–81.
[25] N.M. Deraz, J. Anal. Appl. Pyrolysis 82 (2008) 212–222.
[26] N.M. Deraz, S. Shaban, J. Anal. Appl. Pyrolysis 86 (2009) 173–179.
[27] Zs. Pap, V. Danciu, Zs. Cegléd, Á. Kukovecz, A. Oszkó, A. Dombi, K. Mogyorósi, Appl. Catal. B 101 (2011) 461–470.
[28] H. Zhang, J.F. Banfield, J. Phys. Chem. B 104 (2000) 3481–3487.
[29] R. Jenkins, R.L. Snyder, Introduction to X-ray Powder Diffractometry, John Wiley & Sons, New York, 1996.
[30] J.H. Xu, W.L. Dai, J. Li, Y. Cao, H. Li, H. He, K. Fan, Catal. Commun. 9 (2008) 146–152.
[31] J. Ryu, W. Choi, Environ. Sci. Technol. 42 (2008) 294–300.
[32] S. Livraghi, M.C. Paganini, E. Giamello, A. Selloni, C. Di Valentin, G. Pacchioni, J. Am. Chem. Soc. 128 (2006) 15666.
[33] J. Senthilnathan, L. Philip, Chem. Eng. J. 161 (2010) 83–92.
[34] T. Bezrodna, G. Puchkovska, V. Shymanovska, J. Baran, H. Ratajczak, J. Mol. Struct. 700 (2004) 175–181.
[35] Zs. Pap, L. Baia, K. Mogyorósi, A. Dombi, A. Oszkó, V. Danciu, Catal. Commun., doi:10.1016/j.catcom.2011.10.003.
[36] S. Photong, V. Boonamnuayvitaya, Appl. Surf. Sci. 255 (2009) 9311–9315.
[37] C. Lettmann, K. Hildenbrand, H. Kisch, W. Macyk, W.F. Maier, Appl. Catal. B 32 (2001) 215–227.
[38] C. Di Valentin, E. Finazzi, G. Pacchioni, A. Selloni, S. Livraghi, M.C. Paganini, E. Giamello, Chem. Phys. 339 (2007) 44–56.
[39] J. Yang, H. Bai, X. Tan, J. Lian, Appl. Surf. Sci. 253 (2006) 1988–1994.
[40] R.L. Kurtz, R. Stockbauer, T.E. Madey, Surf. Sci. 218 (1989) 178.
[41] E. Sutter, P. Sutter, E. Fujita, J. Muckerman, Abstracts of the European Materials Research Society Spring Meeting, Nice, France, 2006, p. M-14.
[42] J.M. Cho, J.M. Seo, J.-K. Lee, H. Zhang, R. Lamb, Physica B 404 (2009) 127–130.
[43] K. Mogyorósi, N. Balázs, D.F. Srankó, E. Tombácz, I. Dékány, A. Oszkó, P. Sipos, A. Dombi, Appl. Catal. B 96 (2010) 577–585.